

Maintained Exposure to Spring Water but Not Double Distilled Water in Darkness and Thixotropic Conditions to Weak ($\sim 1 \mu\text{T}$) Temporally Patterned Magnetic Fields Shift Photon Spectroscopic Wavelengths: Effects of Different Shielding Materials

N. J. Murugan^{1,2}, L. M. Karbowski², R. M. Lafrenie^{1,2}, M. A. Persinger^{1,2*}

¹Department of Biology, Laurentian University, Sudbury, Canada

²Biomolecular Sciences Program, Laurentian University, Sudbury, Canada

Email: *mpersinger@laurentian.ca

Received 29 December 2014; accepted 12 January 2015; published 15 January 2015

Copyright © 2015 by authors and Scientific Research Publishing Inc.

This work is licensed under the Creative Commons Attribution International License (CC BY).

<http://creativecommons.org/licenses/by/4.0/>



Open Access

Abstract

Spring water but not double-distilled water was exposed, in darkness, to a temporally patterned weak magnetic field that has been shown to affect planarian behavior and slow the rate of cancer cell proliferation. Exposure to the magnetic field caused a reliable shift in the peak (longer) wavelength of ~ 10 nm for fluorescence emissions and a $\sim 20\%$ increase (~ 100 counts) in fluorescence intensity. Spectral analyses verified a shift of 5 and 10 nm, equivalent to $\sim 1.5 \times 10^{-20}$ J “periodicity” across the measured wavelengths, which could reflect a change in the an intrinsic energy as predicted by Del Giudice and Preparata and could correspond to two lengths of O-H bonds. Wrapping the water sample containers during exposure with copper foil, aluminum foil, or plastic altered these fluorescent profiles. The most conspicuous effect was the elimination of a ~ 280 nm peak in the UV-VIS emission spectra only for samples wrapped with copper foil but not aluminum or plastic. These results suggest that weak magnetic fields produce alterations in the water-ionic complexes sufficient to be reliably measured by spectrophotometry. Because the effect was most pronounced when the spring water was exposed in darkness and was not disturbed the role of thixotropic phenomena and Del Giudice entrapment of magnetic fields within coherent domains of Pol-lack virtual exclusion zones (EZ) may have set the conditions for subsequent release of the energy as photons.

*Corresponding author.

How to cite this paper: Murugan, N.J., *et al.* (2015) Maintained Exposure to Spring Water but Not Double Distilled Water in Darkness and Thixotropic Conditions to Weak ($\sim 1 \mu\text{T}$) Temporally Patterned Magnetic Fields Shift Photon Spectroscopic Wavelengths: Effects of Different Shielding Materials. *Journal of Biophysical Chemistry*, 6, 14-28.
<http://dx.doi.org/10.4236/jbpc.2015.61002>

Keywords

Water, Weak Magnetic Fields, Photon Emissions, Darkness, Thixotropic Phenomena, Copper Shielding, Wavelength Shift, 10^{-20} Joules

1. Introduction

There has been a long and colourful history regarding the potential residual effects of exposing water, particularly when it contains concentrations of ions that approach the characteristics of living systems, to weak magnetic fields [1] because of the unique features of water [2]. Toledo and colleagues [3] reviewed the effects from exposure of water to mT to μ T-intensity magnetic fields, as inferred by measurement of viscosity, enthalpies and surface tension, and suggested intracuster hydrogen bonds were disrupted. Gang *et al.* [4] found that only one hour of exposure to 0.16 T static magnetic fields produced alterations in diffusion velocity of a solute for an additional ~ 6 to ~ 9 hr that was a function of the water volume during exposure. The effect was consistent with the intensity-dependent diminished viscosity reported by Fahidy [5].

Weaker intensity (μ T range), time-varying magnetic fields have been shown to affect ion/ligand binding kinetics when bioeffective waveform parameters were employed [6]-[8]. These alterations in chemical dynamics and biochemical processes are often associated with altered patterns of photon emissions [9]-[11]. Recent theoretical perspectives have extended the concept that water molecules exist as “flickering clusters” [12] with half-lives of $\sim 10^{-11}$ s, several hundred times longer than the period of molecular vibrations. Water containing ions can display coherent domains within which magnetic fields can be “trapped” if the oscillations are optimal [13]. Large polyhedral forms organized from tetrahedral bonded units are considered candidates [14]. The possibility that appropriately patterned extremely low frequency magnetic fields could be trapped within Del Giudice-type coherence domains [13] in water that results in the emission of specific energies and wavelengths within the visible range has been one of our theoretical interests.

We have been investigating the effects of micro Tesla range magnetic fields generated from computer software with configurations that simulate physiological or neuronal patterns. One particular (“frequency-modulated”, decelerating) pattern was shown to produce analgesia in rodents (equivalent to 4 mg/kg of morphine) [15], as well as in snails [16], and to inhibit the growth of several different strains of cancer cells without affecting normal cells [17]. Recently Murugan *et al.* [18] showed that exposure to this pattern for several (3 - 5) days followed by exposure to a modification of a naturally-patterned field produced complete dissolution of populations of planarian. However, these robust phenomena only occurred when the specimens were exposed to the fields in the dark. The interaction between darkness and effective magnetic field exposure upon complex systems has been reported by others [19].

In the pursuit of mechanisms we exposed spring water in the dark to this patterned field and found a conspicuous shift in transmittance counts towards longer wavelengths. Pilot studies indicated the effect was not evident when the water samples were exposed in ambient lighting and that approximately 18 days of magnetic field exposure were required to produce reliable effects. In the present experiments we systematically investigated these phenomena with more precise instrumentation. To discern if different materials could affect the manner in which exposure to the weak magnetic fields could affect the emitted fluorescence of the treated water, we employed spring water (containing a fixed number of cations and anions) and double distilled water and incorporated four different “shielding” conditions: open (no shielding), copper foil, aluminum foil or plastic.

2. Materials and Methods

A total of 176 volumes, each 50 cc, of either spring water or double distilled water contained within 105 cc flint glass jars (9 cm high \times 6 cm diameter) were exposed between two coils as shown in **Figure 1**. Each type of exposure was performed in triplicate; each component of the triplicate was completed on separate days. The two coils were separated by 1 m. Each coil was created by wrapping 305 m of 30 AWG (Belden 9978) wire in a single layer (18 cm wide) around plastic milk crates which were 38 cm \times 33 cm \times 27 cm. The circuit was organized so that one coil would be activated (A) while the other was not activated (NA). Power meter measurements in-



Figure 1. The experimental equipment. When one of the two coils was activated, the proximal containers were location (A), the middle containers were middle (MA), and the distal containers were the non-active (NA). Either coil could be activated.

indicated that the minimum-maximum range in the strengths of the field (RMS) were 4.4 to 11.5 μT for the activated area, 0.3 to 0.6 μT for the middle area (MA), and 0.11 to 0.15 μT for the NA area. For comparison the background intensity for ambient 60 Hz was within the 0.11 - 0.15 μT range. The reference area which also showed that 60 Hz ambient intensity was located 5 m from the two coils.

The magnetic field pattern was generated by a Zenith-386 compute (Model ZF-148-41, Zenith Data Systems, Benton Harbor, MI, USA) computer employing the complex software[®]. A frequency-modulated pattern that has been shown to reduce division rates of cancer cells (by about 1/2) but not normal cells and to affect nociceptive thresholds in rodents was selected. The pattern was produced by converting a series of 849 numbers between 0 and 255 (equivalent to -5 to $+5$ V, where $127 = 0$ V) through a custom constructed digital-to-analogue (DAC) converter (DAC). Each point was generated for 3 ms. The pattern and the spectral power are shown in **Figure 2** and **Figure 3**. This duration was selected because it demonstrates the greatest effect on cell proliferation rates and rodent behavior. Point duration values set less (1, 2 ms) or greater (5, 10 ms) than 3 ms do not produce comparable significant effects [17].

To be comparable with the conditions previously used (in conjunction with the second “sudden commencement geomagnetic field pattern”), to promote the complete dissolution of planaria [18] after 5 days of exposure, all of the present experiments involved exposing the spring or distilled water in the dark (background level as inferred by photomultiplier tube measurements $\sim 10^{-11} \text{ W}\cdot\text{m}^{-2}$). Exposure to even dim ambient lighting reduced the reliability of the effects. Based upon pilot studies where the samples were exposed continuously for 1, 4, 5, 10 and 18 days, we selected 18 days of exposure because it produced the minimal interexperiment variability. However, the effects were apparent after 4 days of exposure.

In an equal numbers of experiments, the containers were exposed to different shielding conditions: They were not wrapped or wrapped with copper foil, aluminum foil, or plastic and then exposed to the three field or reference conditions. Two types of water were employed. Half of the experiments tested spring water (270 ppm HCO_3^- , 71 ppm Ca^{++} , 25 ppm Mg^{++} , 5.9 ppm SO_4^- , 2.7 ppm Cl^- , 2.6 ppm NO_3^- and 1 ppm Na^+) while the other half of the experiments tested double-distilled (DD; ultra-pure, 18 M Ω at 25°C) water.

After the exposure period, the water samples were assessed by fluorescence spectrophotometry. During the entire procedure the samples were not exposed to ambient light until the actual measurement. The samples were also carried in a black box with minimum mechanical perturbation from the exposure room to the measurement room. We had found the incidental “shaking” of the exposed water significantly attenuated the photon-shifting effects. From the time of removal from the field conditions to the initiation of the measurement was about 5 minutes.

For measurements in the Olis RSM 1000 F1 fluorescence spectrophotometer, 1 cc of the water from each condition was placed in a 1 cc quartz cuvette and exposed to a 120 W Xenon arc lamp (excitation source). Measurements were recorded by a DeSa monochromator/photon counter. Ten nanometer scanning intervals between 320 nm and 470 nm for emission were recorded using a dual grating monochromator. On the basis of our results, we also exposed additional samples of 1 cc of water from the various conditions in plastic cuvettes to an Ultrospec 2100 pro uv visible spectrophotometer with a stimulation wavelength of 250 nm. The 1 nm steps ranged

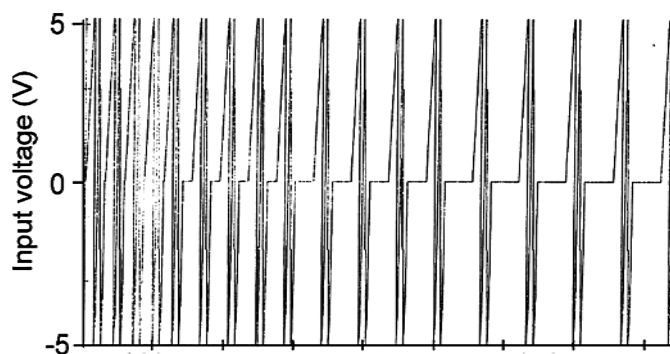


Figure 2. The physiologically-patterned magnetic field composed of 849 points between 0 and 256 that has been associated with significant cellular and biological effects was the one employed in this study. The horizontal axis represents sequence or time. The vertical axis is the voltage output from the computer to the DAC that reflected the transformation of the numbers between 0 and 256 (127 = 0 polarity).

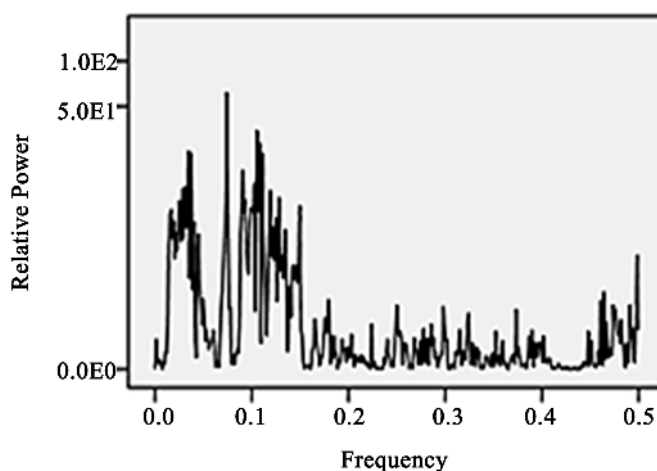


Figure 3. Relative spectral power density of the pattern in Figure 2 as a function of analysis frequency. Actual frequency is the inverse 1 divided by the value multiplied by 3 msec.

from 250 to 500 nm. A monochromator with 1200 lines per mm of aberration corrected for concave grating.

For data analyses, the wavelength that displayed the peak measure of photon transmission was obtained by inspection of the curves. Analyses of variance were completed between the four positions (reference, active, middle, inactive coil), type of shield (open, copper foil, aluminum foil, and plastic) and type of water (spring vs DD). Spectral analyses (PC SPSS 16) were completed for the mean values for triplicates measures of the number of counts per 1 nm between 320 and 470 nm for each of the 32 conditions (4 field conditions, two types of water, and 4 “shielding” conditions). To allow greater comparisons, the z-score values determined from the mean of the triplicates was employed. All analyses were performed using SPSS software for PC. η^2 refers to the amounts of variance in the dependent variable explained by the treatments.

3. Results and Discussion

The general results from these experiments showed that prolonged exposure of water *in the dark* to a temporally patterned electromagnetic field could alter the fluorescent spectrum. The intensities of fluorescence emissions and the maximum emission peaks of the fluorescence spectrum depended on the position of the water in the magnetic field (intensity), the purity of the water, and the presence of different shielding materials during exposure. The means and standard deviations for the peak wavelengths for all conditions are shown in Figure 4.

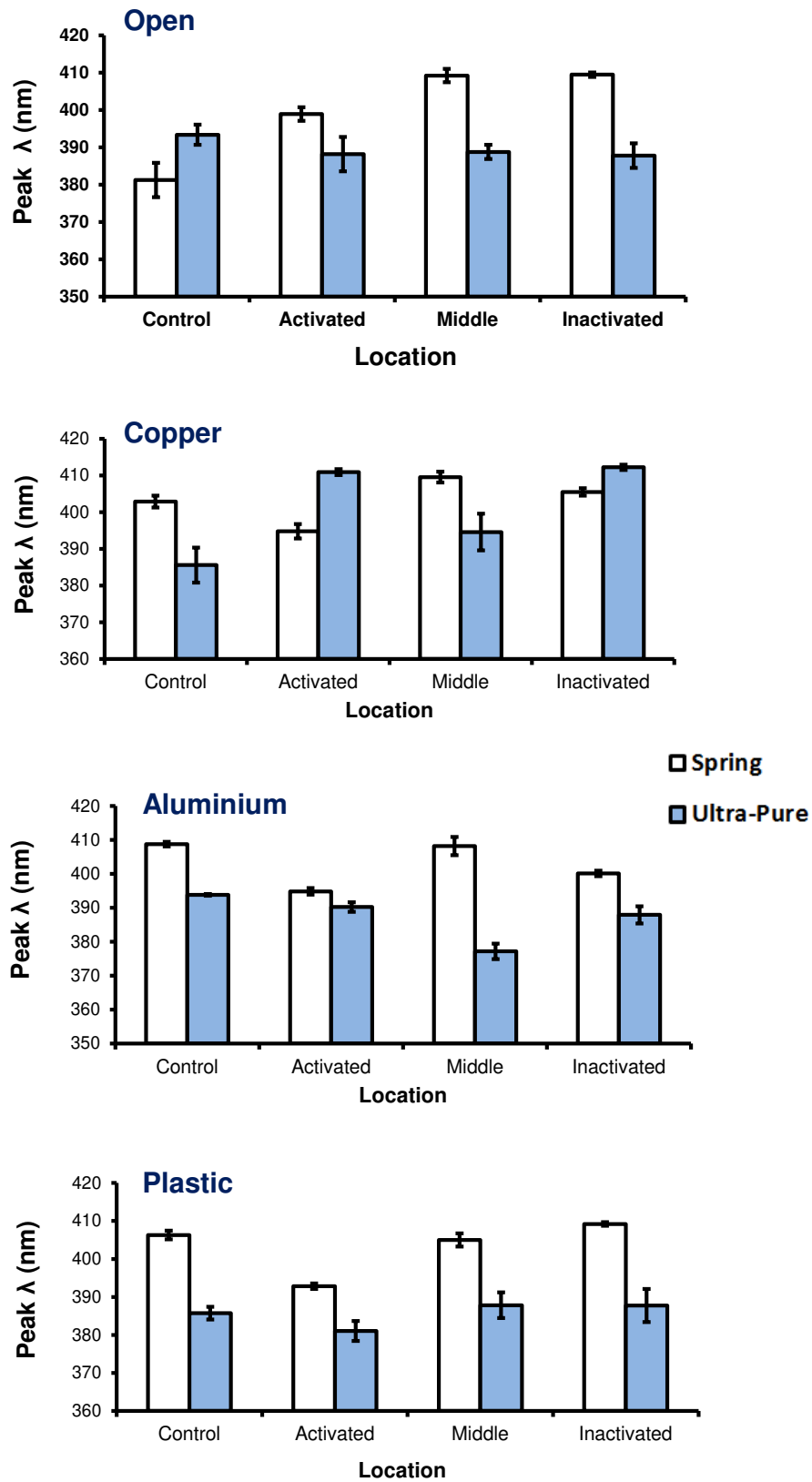


Figure 4. Peak wavelength for maximum numbers of fluorescence counts for spring and ultra-pure (double distilled) water that had been exposed to the different magnetic field conditions and “shielded” (wrapped) with different materials.

3.1. Fluorescence Intensity

The most obvious effect involved the differences in fluorescence emission spectra between spring water and DD water. There were approximately three times the number of photons (counts) emitted from the spring water compared to the DD water. Secondly, the shape of the distribution of counts across the measured wavelengths differed conspicuously. While the fluorescence spectra of the DD water exhibited a linear decrease in counts from the stimulation wavelength, the spring water spectrum exhibited a clear non-linear effect with a maximum peak in intensity between 380 and 440 nm. Systematic magnetic field exposure effects were evident for the spring water but not for the DD water.

The triplicate averages of the total numbers of counts for the spring water exposed for 18 days in darkness to the four field conditions are shown in **Figure 5(a)**. There was a conspicuous shift towards longer emission wavelengths for the spring water that had been exposed to the middle field (0.3 - 0.6 μT) and not activated coil (0.11 - 0.15 μT) conditions (peak around 418 nm) compared to the active field (4.4 - 11.5 μT) and reference conditions (peak around 400 nm). Between 420 and 475 nm, the intensity of emitted fluorescence for the middle field and not activated field was about 150 counts per unit wavelength higher than for the reference and active field conditions. Neither the non-linear effect nor the differential field condition effects were noted in the DD water (**Figure 5(b)**). These results clearly showed that the weaker intensity, patterned field (below 0.6 μT , 6 mG) that was presented in addition to the background 60 Hz ambient intensities produced the greatest shift in wavelength. The spring water exposed to the not activated field produced discernibly higher fluorescence intensity counts between 460 and 470 nm.

The effects of adding the three different shielding materials during the 18 days of dark magnetic field exposures to the produced fluorescence counts produced by the spring and DD water are shown in **Figures 6-8**. The results for each type of water for each type of shielding are presented in the same graph to facilitate comparison. For the copper foil shielding (**Figure 6**), the most conspicuous effect (420 to 440 nm) involved samples exposed in the area adjacent to the inactive coil and for spring water only. For the aluminum foil (**Figure 7**) shielding the middle region showed more fluorescence emission counts than the inactive coil region between 420 to 440 nm although both were elevated above the active and reference regions. The plastic shielding produced a markedly attenuated effect within a narrow band of 420 to 430 nm (**Figure 8**).

3.2. Peak Wavelength Effects

The peak wavelengths, the values where fluorescence intensities of the spectrum were maximal for each experimental condition, were shown in **Figure 4**. The general results were clear for all experiments combined (**Table 1**). Two way analysis of variance indicated a statistically significant difference in fluorescence emission for the two types of water [$F(1,168) = 63.03$, $p < 0.001$; $\eta^2 = 24\%$]. There was a significant interaction between the location of the beakers (field strength) from the activated coil and type of water [$F(3,168) = 6.65$, $p < 0.001$; $\eta^2 = 8\%$]. When analyzed according to each of the types of “shielding” during exposure, the effects of the magnetic field exposure upon the peak fluorescence emission wavelength was very clear.

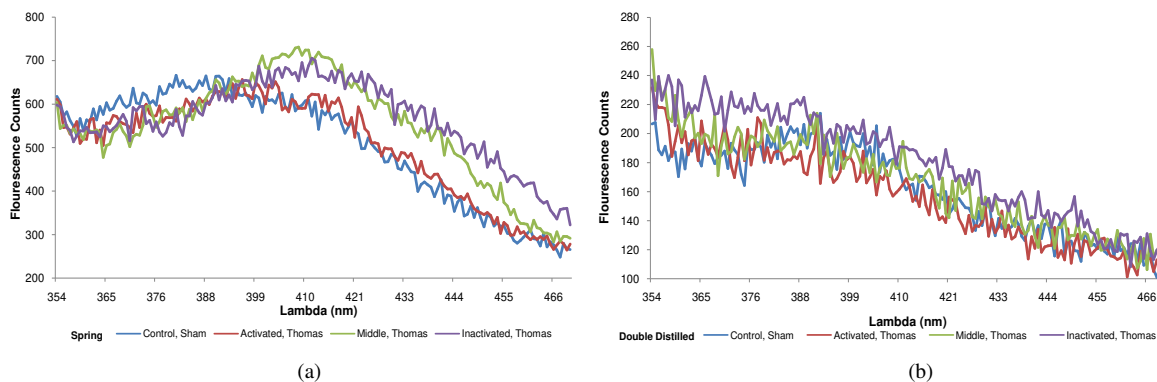


Figure 5. Number of counts by fluorescence spectrophotometry for spring (a) or double distilled (b) water that had been exposed to the reference (blue), active area (red), middle area (green) and inactive area (purple). Note the shift by approximately 10 nm for the latter two conditions for the spring water.

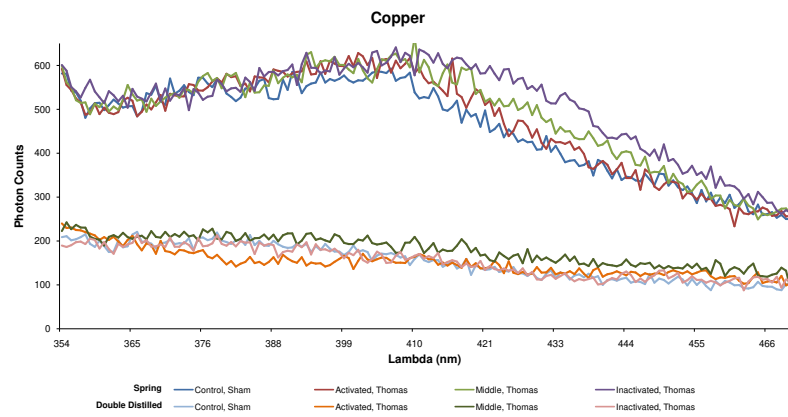


Figure 6. Photon counts from spring water (upper curves) or double distilled (lower section of graph) water that had been exposed to the four conditions of magnetic field but wrapped with copper foil.

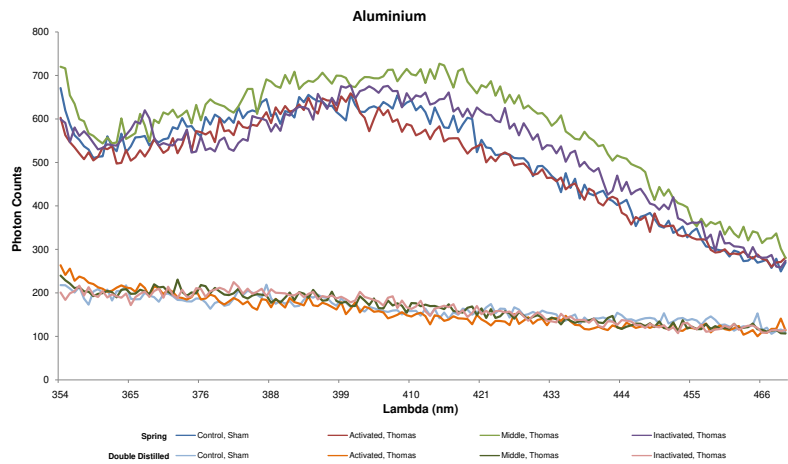


Figure 7. Photon counts from spring (upper curves) or double distilled (lower lines) water that had been exposed to the various magnetic field treatments but wrapped with aluminium foil.

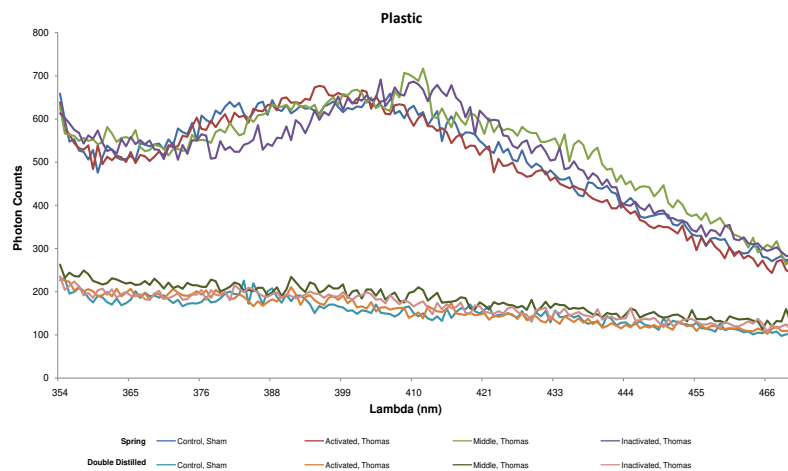


Figure 8. Photon counts from spring (upper curves) or double distilled (lower lines) water that had been exposed to the various magnetic field treatments but wrapped with plastic.

Table 1. Means and standard deviations for the peak wavelengths (in nm) of numbers of photon counts by fluorescent spectrophotometry for the two types of water, field conditions, and shielding materials.

		Water Type							
		Spring Water				Double-Distilled Water			
		Field Condition	Control	Activated	Middle	Inactivated	Control	Activated	Middle
Shielding Condition	Open	381.25 (4.6)	398.90 (1.8)	409.20 (1.8)	409.45 (0.6)	393.33 (2.7)	388.17 (4.6)	388.75 (1.9)	387.75 (3.3)
	Copper	402.90 (1.6)	394.80 (2.0)	409.55 (1.5)	405.50 (1.0)	385.50 (4.8)	410.90 (0.8)	394.5 (5.0)	412.25 (0.7)
	Aluminium	408.75 (0.7)	394.85 (1.0)	408.2 (2.7)	400.15 (0.8)	393.833 (0.3)	390.25 (1.4)	377.16 (2.2)	387.91 (2.5)
	Plastic	406.3 (1.1)	392.85 (0.7)	405 (1.7)	409.2 (0.5)	385.75 (1.7)	381.0833 (2.6)	387.83 (3.4)	387.75 (4.4)

As shown in **Table 1**, field exposures in non-shielded containers produced a strong shift in emission wavelength [$F(3,16) = 24.81$] that explained 82% of the variance (equivalent to an $r = 0.91$). *Post hoc* analysis indicated that the emission spectra of the spring water exposed to the middle and non-activated loci displayed significantly longer peak wavelengths (~409 nm) than either the control (~381 nm) or the activated (~399 nm) locations. The diminished energy difference for the wavelength between the activated and two other loci exposed to the field was equivalent to 1.4×10^{-20} J. On the other hand, the DD water exposed in the same areas did not differ significantly for the peak emission wavelength [$F(3,20) = 0.55$, $p > 0.05$].

The energy difference of 1.4×10^{-20} J as reflected by the shift in wavelength may be useful for discerning mechanism. The ratio of the magnetic moment of a proton (1.41×10^{-26} A·m²) and unit charge (1.6×10^{-19} A·s) is a diffusivity aggregate of units (0.88×10^{-7} m²·s⁻¹). When multiplied by the viscosity of water (8.94×10^{-4} kg·m⁻¹·s⁻¹ at biological temperatures) the force is in the order of 7.87×10^{-11} kg·m⁻¹·s⁻². When applied across the typical length of two O-H bonds spanning between water molecules (1.92×10^{-10} m), the functional energy would be $\sim 1.5 \times 10^{-20}$ J [19].

On the other hand, the emission spectra of both the spring water [$F(3,16) = 16.19$, $p < 0.001$; $\eta^2 = 0.75$] and DD water [$F(3,20) = 13.67$, $p < 0.001$; $\eta^2 = 0.67$] wrapped in copper foil displayed a difference in fluorescence intensity depending on the location of the containers (effectively field strength). For the spring water that had been exposed to the active coil, the emission spectra showed a marked elevation in wavelength at 395 nm compared to the control, middle, or not activated areas where the maximal values were seen at 403 to 410 nm. *Post hoc* analysis indicated that these peak wavelengths for the control and middle area did not differ significantly from each other but both differed from the peak wavelength for activated and non-activated loci that did not differ from each other.

In the presence of aluminum shielding, both the spring water [$F(3,16) = 19.02$, $p < 0.001$; $\eta^2 = 14\%$] and the DD water displayed differences in peak wavelengths for the emission spectra. *Post hoc* analyses indicated that for the spring water the peak wavelengths for the active and NA locations did not differ from each other (395 - 400 nm) but were significantly lower than those exposed to the control or middle regions (408 nm) that did not differ significantly from each other. Only the DD water within the middle region displayed a shorter peak wavelength (377 nm) than the other three locations (388 to 393 nm) that did not differ significantly from each other.

The fluorescence emission spectra of the spring water shielded by plastic exhibited significant differences in peak wavelength depending on the different locations [$F(3,16) = 41.06$, $p < 0.01$; $\eta^2 = 50\%$]. *Post hoc* analysis indicated that the water exposed to the active region displayed shorter peak wavelengths (393 nm) than the other three locations (405 to 409 nm) that did not differ significantly from each other. However, there were no significant differences in peak wavelengths for the DD shielded by plastic as a function of the four locations [$F(3,20) = 1.00$, $p > 0.05$].

3.3. Spectral Power Density Analyses

The results of the spectral analyses for the fluorescence emission spectra for water (spring and DD) exposed to the different positions in the magnetic field and different shielding conditions (open, copper, aluminum, or plastic) versus the z-scores of the total counts revealed intrinsic periodicities within the wavelengths. The phenome-

na were most evident in the spring water exposed to the four field conditions *without* any shielding. As shown in **Figure 9**, the spring water exposed to the active field area exhibited a relative increase in power around 10 nm and 5 nm. **Figure 10** shows the results of the same analysis for the water from the reference area and indicates the expected exponential decay. The conspicuous profile for the active field exposure was not evident for spring water exposed to the MA or IA, although an increase in relative spectral power is discernable visibly for 9 to 10 nm repetitions of wavelength.

At face value the results suggest that exposure to the patterned magnetic field resulted in the display of an intrinsic molecular structure within the spring water and its constituents. This pattern resembled a standing wave across the 320 to 470 nm, 1 nm increments and appears to reflect the width of a plasma cell membrane. In addi-

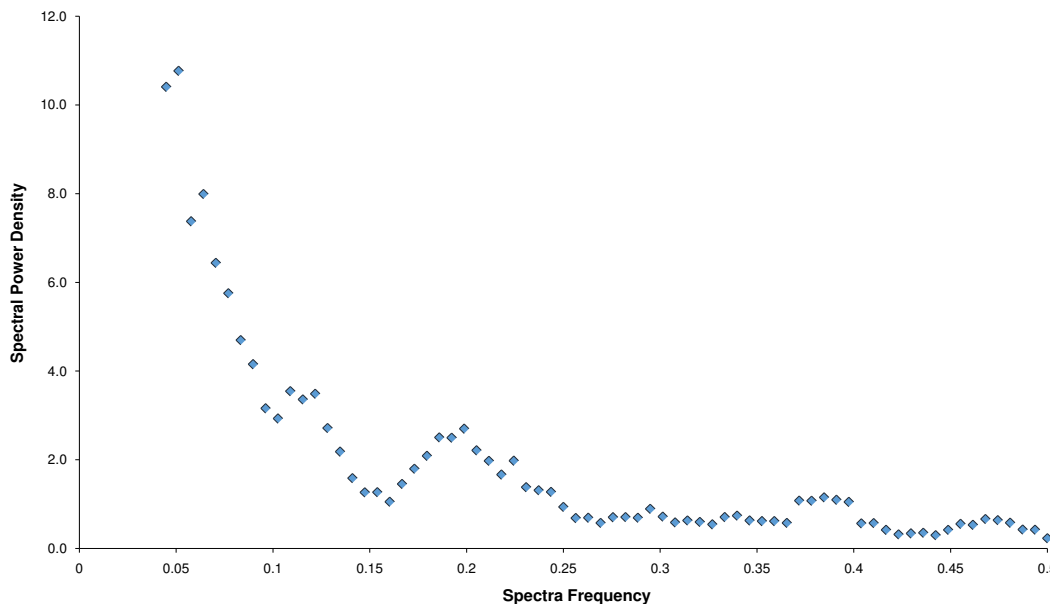


Figure 9. Spectral power density of numbers of photon counts as a function of wavelength for water exposed to the active magnetic field area. In this instance 1 divided by the value in the x-axis reflects the wavelength. Note the peaks around 10, 5, and 2.5 nm.

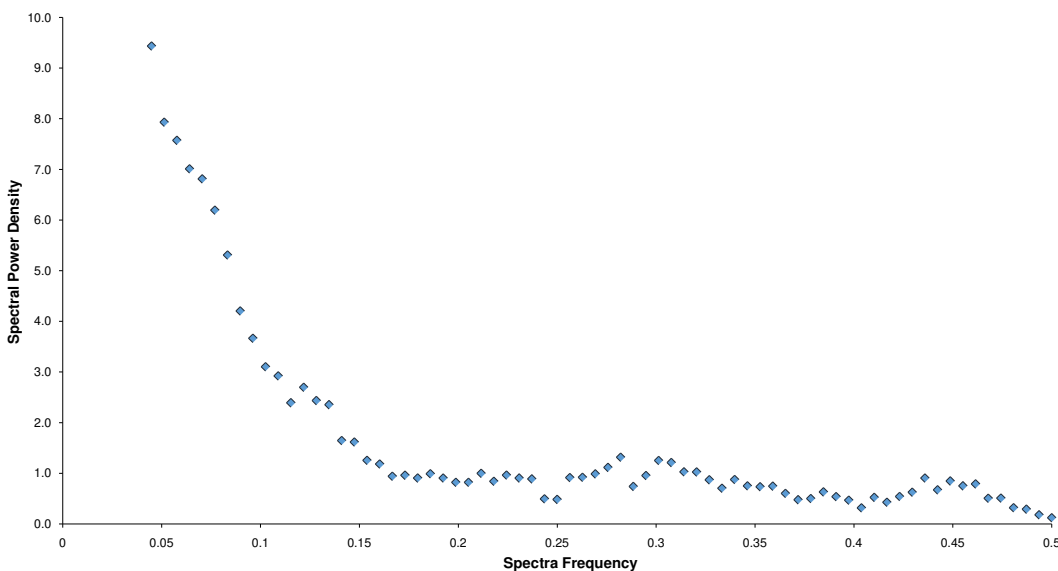


Figure 10. Spectral power density of numbers of photon counts as a function of wavelength for water exposed to the control conditions. Not absence of the enhanced power spectra density around 10 and 5 nm.

tion, the ~10 nm, 5 nm, and 2.5 nm peaks are similar to the quantum steps seen in cell systems when examining the spacing of actin monomers within activated myofibrils. Pollack [20] found these peaks were integer multiples of actin-monomer spacing.

3.4. UV-VIS Spectroscopy

Over the last decade of research with physical, chemical and biological systems that involved shifts in pH, photon emissions, and proton-driven reactions we [21] have noted that the efficacy of the pattern of the applied magnetic field is more related to its spectral characteristics and power densities (Figure 3) than to intensity, *per se*, at least within biologically-effective ranges. The mean of the first peak in power density for the magnetic field presented at 3 ms which was used in this study as shown in Figure 3 is around 8 Hz. Although not frequently employed for analyses of weak fields, we think it is a potentially relevant. The difference between the magnetic moments for the electron's spin and orbit ($1.07 \times 10^{-26} \text{ J}\cdot\text{T}^{-1}$) multiplied by $0.5 \times 10^{-7} \text{ T}$ (the maximum intensity in MA) is $5.35 \times 10^{-33} \text{ J}$. When divided by Planck's constant the emergent frequency is ~8 Hz.

We selected the spin-orbit magnetic moment difference because of its theoretical value in the relationship between photon emission and the ephemeral features of the fourth quantum number (spin) that defines location. However this net difference between the magnetic moments for the spin and orbit of an electron is very similar to the proton magnetic moment ($1.41 \times 10^{-26} \text{ A}\cdot\text{m}^2$). As mentioned previously the ratio between this value and the unit charge is $0.88 \times 10^{-7} \text{ m}^2\cdot\text{s}^{-1}$ and when multiplied by the mass of the proton is $1.47 \times 10^{-34} \text{ kg}\cdot\text{m}^2\cdot\text{s}^{-1}$. When 8 Hz is applied the energy is within the range of the 10^{-33} J associated with spin-orbit levels coupled with this frequency magnetic field [22] [23]. Although this convergence does not prove a functional connection it does suggest shared frequency and energy levels by which the magnetic fields could directly interact with water structure.

Consequently we decided to discern if a very narrow and enhanced peak in transmittance would be evident if a UV pulse was generated through the spring water covered with different shielding material that had been exposed to this intensity (the MA). The results are shown in Figure 11. For the plastic and aluminum foil conditions the marked enhancement occurred between 275 and 305 nm only for the spring water exposed to the 0.3 to 0.6 μT fields and neither the strongest (active) or weakest (inactive) coil. However this was not observed for the spring water that had been shielded with the copper foil. Copper ions in solution rather than wrapped around water through which magnetic fields are penetrating, have been shown to dramatically decrease fluorescence intensity. In fact this conspicuous peak was completely eliminated.

4. General Discussion

These results indicate that the processes who characteristics were hypothesized or described by Pollack and his colleagues [2] [20] and Del Giudice and his colleagues [13] could be explored experimentally by examining photon emission after exposure of spring water to weak magnetic fields. The pattern employed in this experiment was a variant of a frequency and phase-modulated field that had been shown to affect the behaviour of invertebrates and vertebrates [15] [16]. We had also shown experimentally that this patterned field affected the drift in pH of spring water after several hours of exposure. These shifts in pH occurred as brief 0.02 increments towards alkalinity with durations in the order of 20 to 40 ms [24].

The two important conditions to produce the robust effect of increasing the photon emissions and the shifts in wavelengths were exposures of the water volumes in a very dark environment ($10^{-11} \text{ W}\cdot\text{m}^{-2}$) for more than 10 days and the minimal mechanical disturbance of that exposed water before the spectrophotometric measurement. Verdel and Bukovec [25] have described the thixotropy of water which refers to the increased viscosity and gel-like behaviours of water which develop spontaneously over time. The phenomenon of increased viscosity emerges when ions and hydrophilic surfaces are present and diminishes during mechanical stimulation.

Their review [25] suggested that the emergence of a structured network of hydrogen bonds between water molecules and ions in aqueous solutions that are not disturbed for protracted periods was a significant contributor to the phenomenon. The primary hypothesis was that thixotropy or the alternative order of hydrogen bond networks facilitated faster proton transfer in protracted, non-disturbed solutions that could involve Grotthuss mechanisms. Presumed OH-bond stretching and bending of water molecules within the femtosecond range is assumed to be followed by dissipation of that energy into the network of hydrogen bonds for a few picoseconds, or, about the life time of a hydronium ion [26].

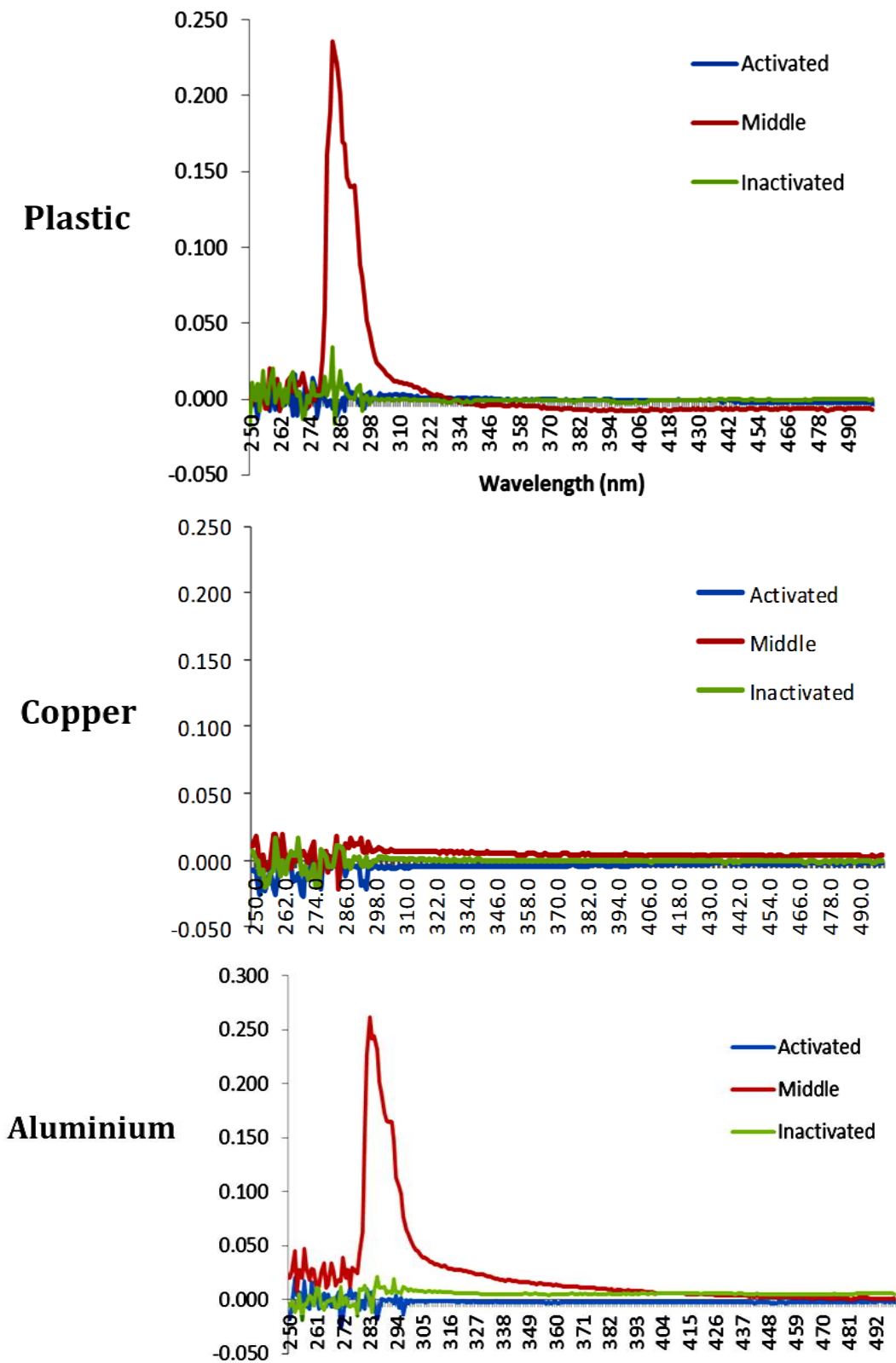


Figure 11. Relative measures for emission (uv) for spring water that had been exposed to the active, middle or inactive areas while being wrapped (“shielded”) with either plastic, copper, or aluminium foil. Note the marked enhancement of emission around 280 nm for the plastic and aluminium foil wrapping that was eliminated by copper foil.

In several elegant experiments, Pollack *et al.* [2] [20] have demonstrated the differentiation between bulk water and interfacial water near surfaces of hydrophilic materials. Within these Exclusion Zones (EZ) solutes are minimal and the layer of protons can be equivalent to 150 to 200 mV near the nucleating surface. The emergence of these zones required several minutes to hours and were associated with a gradual expansion due to raising internal “pressure” from the protons inside the “vesicle” of water. Sedlak [27] estimated that the number of molecules per domain within several types of aqueous systems ranged between 10^3 and 10^8 . Minutes to weeks were required for supramolecular structures to emerge and to achieve asymptote. After about 80 days the domains appeared to be stable with diameters between 30 and 500 nm.

According to Chai *et al.* [28], absorption of energy within the Pollack Exclusion Zones in aqueous solutions peaked around 270 nm. The peak was very similar for a variety of solutions that included salts, L-lysine, D-alanine, D-glucose and sucrose. On the other hand the fluorescent properties of these solutions displayed peak emissions of energy around 480 and 490 nm following excitation by different wavelengths. We found that emission spectra for water that had been exposed to the magnetic field (0.3 to 0.6 μ T) in the position between the active and inactive coil generated a conspicuous increase in photon emission power density between 275 and 305 nm (peak = 280 nm).

The very remarkable phenomenon associated with this conspicuous peak in UV emission from water exposed to this narrow band intensity of the patterned magnetic field was its complete diminishment if the water had been wrapped during the exposures with copper (Figure 11) but not other materials such as plastic or aluminum. Because we measured the magnetic field’s presence within the confines of the copper wrapping, total impedance of penetration of the flux lines is not a likely mechanism. We have been pursuing this conspicuous phenomenon from the perspective of the Aharonov-Bohm effect.

We have encountered the emergence of 10^{-20} J as a fundamental unit or packet of energy in several contexts that range from cosmological to local applications [29]-[32]. For example the energy associated with the separation between the potassium ions along the surface of a plasma cell membrane that has been attributed to the resting membrane potential as well as the neuronal action potential is about 10^{-20} J. Comparable values are associated with sequestering of a ligand to a receptor [33]. It is also the quantity of energy that emerges when the total force of the universe is divided by the numbers of Planck Voxels (Planck’s Length cubed) is applied across the wavelength of the neutral hydrogen line [30].

Our measurement of a shift of 10 nm, the approximate width of a plasma cell membrane, and the associated energy of $\sim 1.4 \times 10^{-20}$ J for this difference in the 400 nm range (the interface between UV and Visible Light) could reveal some of the intrinsic parameters associated with the molecular and bonding structures of undisturbed water exposed in the dark to weak, physiologically-patterned magnetic fields. Even spectral analyses of the power densities distributed across the band of wavelengths for the photon emissions from the magnetic field exposed water revealed this “standing spatial wave” of about 10 nm.

The results are directly applicable to the coherent dynamics in water described by Del Giudice and Preparata [13] who extended the Dicke Hamilton expression for special properties that emerge in matter at specific atomic densities and temperatures. This spontaneous phase transition, often described as the Superradiant Phase Transition (SPT), exhibits the capacity to embed or “trap” electromagnetic fields within an atomic ensemble that is oscillating in phase with atomic transitions between ground states and excited conditions. They estimated the gap energy in a system of N two-level atoms would be:

$$E = hc \cdot \lambda^{-1} \quad (1)$$

where h is Planck’s constant, c is the velocity of light and λ is the wavelength involved. If the difference between peak wavelength ($\lambda = 381$ nm) for the sham field exposed water and the peak wavelengths (between 399 to 409 nm) for magnetic field exposed samples is calculated, the difference in energies would be $\sim 1.2 \times 10^{-20}$ J which is within measurement error of what we obtained in the experimental setting. These results could suggest that the applied magnetic fields were trapped within the SPT facilitated by combinations of exposure to darkness and thixotropic processes. The energy associated with these “trapped fields” was manifested by the 10 nm displacement of wavelengths of photons within the narrow band interface between the UV and visible boundary.

If these phenomena are to be related to quantum effects there should be quantitative convergence between the most fundamental features of the latter and the absorption of the former. Liquid water absorbs strongly at wavelengths between 2.9 and 3.25 μ m [28]. This is assumed to correspond to the stretching of the O-H bond from which the energy attributed to the longer duration hydronium ion originates. The simple average of these wave-

lengths is 3.08 μm which we suggest is not spurious.

Precisely half this value, 1.55 μm , is within error measurement of the energy associated with the quantum involved with the removal of one nucleus from the other in a hydrogen molecule. The frequency is about 1.91×10^{14} Hz and is the same order of magnitude as that estimated for atomic or nuclear vibration of hydrogen from the perspective of molecular heat [34]. Bohr had noted that there was no absorption of energy within this wavelength in hydrogen gas which was attributed to the symmetrical structure of the hydrogen molecule and the significant ratio between the frequencies corresponding to displacements of electrons (about 3.7×10^{15} Hz) and nuclei (1.91×10^{14} Hz). The observation that water exhibits this absorption may indicate that the interface for a special type of electron-proton interaction may exist as a special condition within this compound. It has been considered by Voeikov and Del Giudice to be the bases of the living state [35]. We have considered water to be “the Solvent of Life”.

5. Conclusion

In conclusion spring water displayed a non-linear scatter of spectrophotometric transmittance as a function of wavelength while double-distilled water exhibited the expected linear decay as a function of distance from the stimulation wavelength. Exposure of spring water but not double distilled water to a temporally patterned weak magnetic field in the dark for about two weeks produced several classes of reliable effects revealed by photon transmission. The weakest magnetic fields in the order of μT produced approximately 10 nm shift in peak transmittance towards longer wavelengths. Spectral analysis confirmed the presence of 5 and 10 nm periodicities in spectral density across the measured range but this was evident only with the strongest (4 - 11 μT) magnetic intensity. Concomitant exposure to different types of wrapping around the water samples indicated that copper foil eliminated the ~ 280 nm spike in transmission compared to aluminum foil or plastic as inferred by UV-VIS spectrometry. These results indicate there is a rich complexity of subtle molecular changes within water, particularly spring water, exposed to this temporally patterned magnetic field.

Acknowledgements

The authors thank Dr. Blake T. Dotta for his technical expertise and Dr. S. S. Siemann for the use of his equipment.

References

- [1] DeMeo, J. (2011) Water as a Resonant Medium for Unusual External Environmental Factors. *Water*, **3**, 1-47.
- [2] Pollack, G.H., Figueroa, Z. and Zhao, Q. (2009) Molecules, Water and Radiant Energy: New Clues to the Origin of Life. *International Journal of Molecular Sciences*, **10**, 1419-1429. <http://dx.doi.org/10.3390/ijms10041419>
- [3] Toledo, E.J., Ramalo, Z.M. and Magriotis, J. (2008) Influence of Magnetic Field on Physical-Chemical Properties of the Liquid Water: Insights from Experimental and Theoretical Models. *Journal of Molecular Structure*, **888**, 409-415. <http://dx.doi.org/10.1016/j.molstruc.2008.01.010>
- [4] Gang, N., St-Pierre, L.S. and Persinger, M.A. (2012) Water Dynamics Following Treatment by One Hour of 0.16 Tesla Static Magnetic Fields Depends on Exposure Volume. *Water*, **3**, 122-131.
- [5] Fahidy, T.Z. (1999) The Effects of Magnetic Fields on Electrochemical Processes. In: Conway, B.E., Bockris, J.O.M. and White, R.E., Eds., *Modern Aspects of Electrochemistry*, Plenum Press.
- [6] Pilla, A.A., Muehsam, D.J., Markov, M.S. and Siskin, F.F. (1999) EMF Signals and Ion/Ligand Binding Kinetics: Prediction of Bioeffective Waveforms Parameters. *Bioelectrochemistry and Bioenergetics*, **48**, 27-34. [http://dx.doi.org/10.1016/S0302-4598\(98\)00148-2](http://dx.doi.org/10.1016/S0302-4598(98)00148-2)
- [7] Blank, M. and Soo, L. (1998) Frequency Dependence of Cytochrome Oxidase Activity in Magnetic Fields. *Bioelectrochemistry and Bioenergetics*, **46**, 139-143. [http://dx.doi.org/10.1016/S0302-4598\(98\)00126-3](http://dx.doi.org/10.1016/S0302-4598(98)00126-3)
- [8] Mullins, J.M., Litovitz, T.A., Penafiel, M., Desta, A. and Krause, D. (1998) Intermittent Noise Affects EMF-Induced ODC Activity. *Bioelectrochemistry and Bioenergetics*, **44**, 237-242. [http://dx.doi.org/10.1016/S0302-4598\(97\)00073-1](http://dx.doi.org/10.1016/S0302-4598(97)00073-1)
- [9] Cifra, M., Fields, J.Z. and Farhadi, A. (2011) Electromagnetic Cellular Interactions. *Progress in Biophysics and Molecular Biology*, **105**, 223-246. <http://dx.doi.org/10.1016/j.pbiomolbio.2010.07.003>
- [10] Dotta, B.T., Buckner, C.A., Cameron, D., Lafrenie, R.M. and Persinger, M.A. (2011) Biophoton Emissions from Cell Cultures: Biochemical Evidence for the Plasma Membrane as the Primary Source. *General Physiology and Biophysics*, **30**, 301-309.

- [11] Dotta, B.T. and Persinger, M.A. (2012) Doubling of Local Photon Emissions When Two Simultaneous, Spatially-Separated, Chemiluminescent Reactions Share the Same Magnetic Field Configurations. *Journal of Biophysical Chemistry*, **3**, 72-80. <http://dx.doi.org/10.4236/jbpc.2012.31009>
- [12] House, C.R. (1974) *Water Transport in Cells and Tissues*. Edward Arnold, London.
- [13] Del Giudice, E. and Preparata, G. (1994) Coherent Dynamics in Water as a Possible Explanation of Biological Membranes Formation. *Journal of Biological Physics*, **20**, 105-116. <http://dx.doi.org/10.1007/BF00700426>
- [14] Roy, R., Tiller, W.A. and Hoover, M.R. (2005) The Structure of Liquid Water: Novel Insights from Materials Research. *Materials Research Innovation*, **9-4**, 1433-075x.
- [15] Martin, L.J., Koren, S.A. and Persinger, M.A. (2004) Thermal Analgesic Effects from Weak, Complex Magnetic Fields and Pharmacological Interactions. *Pharmacology, Biochemistry and Behavior*, **78**, 1219-1224. <http://dx.doi.org/10.1016/j.pbb.2004.03.016>
- [16] Thomas, A.W., Kavaliers, M., Prato, F.S. and Ossenkopp, K.P. (1997) Antinociceptive Effects of Pulsed Magnetic Fields in the Land Snail. *Neuroscience Letters*, **222**, 107-110. [http://dx.doi.org/10.1016/S0304-3940\(97\)13359-6](http://dx.doi.org/10.1016/S0304-3940(97)13359-6)
- [17] Buckner, C. (2001) *Effects Electromagnetic Fields on Biological Processes Are Spatial and Temporal-Dependent*. Ph.D. Dissertation, Laurentian University, Sudbury.
- [18] Murugan, N.J., Karbowski, R.M., Lafrenie, R.M. and Persinger, M.A. (2013) Temporally-Patterned Magnetic Fields Induce Complete Fragmentation in Planaria. *PLOS ONE*, **8**, e61714.
- [19] Prato, F.S., Kavaliers, M., Thomas, A.W. and Ossenkopp, K-P. (1998) Modulatory Actions of Light on the Behavioural Responses to Magnetic Fields by Land Snails Probably Occur at the Magnetic Field Detection Stage. *Proceedings from the Royal Society of London*, **265**, 367-373. <http://dx.doi.org/10.1098/rspb.1998.0304>
- [20] Pollack, G.H. (2003) The Role of Aqueous Interfaces in the Cell. *Advances in Colloid and Interface Science*, **103**, 173-196. [http://dx.doi.org/10.1016/S0001-8686\(02\)00095-7](http://dx.doi.org/10.1016/S0001-8686(02)00095-7)
- [21] Dotta, B.T., Vares, D.E.A., Buckner, C.A., Lafrenie, R.M. and Persinger, M.A. (2014) Magnetic Configurations Corresponding to Electric Field Patterns That Evoke Long-Term Potentiation Shift Power Spectra of Light Emissions from Microtubules from Non-Neural Cells. *Open Journal of Biophysics*, **4**, 112-118. <http://dx.doi.org/10.4236/ojbiphy.2014.44013>
- [22] Dotta, B.T., Lafrenie, R.M., Karbowski, L.M. and Persinger, M.A. (2014) Photon Emission from Melanoma Cells during Brief Stimulation by Patterned Magnetic Fields: Is the Source Coupled to Rotational Diffusion within the Membrane? *General Physiology and Biophysics*, **33**, 63-73. <http://dx.doi.org/10.4149/gpb.2013066>
- [23] Persinger, M.A. (2014) Quantitative Convergence between Physical-Chemical Constants of the Proton and the Properties of Water: Implications for Sequestered Magnetic Fields and a Universal Quantity. *International Letters of Chemistry, Physics and Astronomy*, **2**, 1-10.
- [24] Murugan, N.J., Karbowski, L.M. and Persinger, M.A. (2014) Serial pH Increments (~20 to 40 Milliseconds) in Water during Exposures to Weak, Physiologically Patterned Magnetic Fields: Implications for Consciousness. *Water*, **6**, 45-60.
- [25] Verdel, N. and Bukovec, P. (2014) Possible Further Evidence for the Thixotropic Phenomena of Water. *Entropy*, **16**, 2146-2160. <http://dx.doi.org/10.3390/e16042146>
- [26] Decoursey, T.E. (2003) Voltage-Gated Proton Channels and Other Proton Transfer Pathways. *Physiology Reviews*, **83**, 475-579.
- [27] Sedlak, M. (2013) Large Scale Supramolecular Structure in Solutions of Low Molar Mass Compounds and Mixtures of Liquids: II. Kinetics of the Formation and Long Time Stability. *Journal of Physical Chemistry B*, **110**, 4339-4345. <http://dx.doi.org/10.1021/jp056934x>
- [28] Chai, B., Yook, H. and Pollack, G.H. (2009) Effect of Radiant Energy on Near-Surface Water. *Journal of Physical Chemistry*, **113**, 13953-13958. <http://dx.doi.org/10.1021/jp908163w>
- [29] Persinger, M. (2014) Convergence of Numbers of Synapses and Quantum Foci within Human Brain Space: Quantitative Implications of the Photon as a Source of Cognition. *International Letters of Chemistry, Physics and Astronomy*, **11**, 59-66.
- [30] Persinger, M.A., Koren, S.A. and Lafreniere, G.F. (2008) A Neuroquantologic Approach to How Human Thought Might Affect the Universe. *Neuroquantology*, **6**, 262-271. <http://dx.doi.org/10.14704/nq.2008.6.3.182>
- [31] Persinger, M.A. and Koren, S.A. (2013) Dimensional Analyses of Geometric Products and the Boundary Conditions of the Universe: Implications for a Quantitative Value for Latency to Display Entanglement. *The Open Astronomy Journal*, **6**, 10-13. <http://dx.doi.org/10.2174/1874381101306010010>
- [32] Persinger, M.A. (2014) Discrepancies between Predicted and Observed Intergalactic Magnetic Field Strengths from the Universe's Total Energy: Is It Contained within Submatter Spatial Geometry? *International Letters of Chemistry, Physics*

and Astronomy, **11**, 18-23.

- [33] Persinger, M.A. (2010) 10-20 Joules as a Neuromolecular Quantum in Medicinal Chemistry: An Alternative Approach to Myriad Molecular Pathways? *Chemical Medicinal Chemistry*, **17**, 3094-3098.
- [34] Lewis, W.C. (1921) *A System of Physical Chemistry: Volume III Quantum Theory*. Longmans, Green and Company, Bombay, p.115-117.
- [35] Voeikov, V.L. and Del Giudice, E. (2009) Water Respiration—The Basis of the Living State. *Water*, **1**, 52-75.

Scientific Research Publishing (SCIRP) is one of the largest Open Access journal publishers. It is currently publishing more than 200 open access, online, peer-reviewed journals covering a wide range of academic disciplines. SCIRP serves the worldwide academic communities and contributes to the progress and application of science with its publication.

Other selected journals from SCIRP are listed as below. Submit your manuscript to us via either submit@scirp.org or [Online Submission Portal](#).

